

# A Possible Dynamically Cold Classical Contact Binary: (126719) 2002 CC<sub>249</sub>

Audrey Thirouin on and Scott S. Sheppard on Scott S. Sheppard Lowell Observatory, 1400 W Mars Hill Road, Flagstaff, Arizona, 86001, USA; thirouin@lowell.edu Department of Terrestrial Magnetism (DTM), Carnegie Institution for Science, 5241 Broad Branch Road NW, Washington, District of Columbia, 20015, USA; ssheppard@carnegiescience.edu Received 2017 August 30; revised 2017 October 26; accepted 2017 October 27; published 2017 November 21

#### Abstract

Images of the Kuiper Belt object (126719) 2002  $CC_{249}$  obtained in 2016 and 2017 using the 6.5 m *Magellan-Baade Telescope* and the 4.3 m Discovery Channel Telescope are presented. A light curve with a periodicity of 11.87  $\pm$  0.01 hr and a peak-to-peak amplitude of 0.79  $\pm$  0.04 mag is reported. This high amplitude double-peaked light curve can be due to a single elongated body, but it is best explained by a contact binary system from its U-/V-shaped light curve. We present a simple full-width-at-half-maximum test that can be used to determine if an object is likely a contact binary or an elongated object based on its light curve. Considering that 2002  $CC_{249}$  is in hydrostatic equilibrium, a system with a mass ratio  $q_{\min} = 0.6$ , and a density  $\rho_{\min} = 1$  g cm<sup>-3</sup>, or less plausible a system with  $q_{\max} = 1$ , and  $\rho_{\max} = 5$  g cm<sup>-3</sup> can interpret the light curve. Assuming a single Jacobi ellipsoid in hydrostatic equilibrium and an equatorial view, we estimate  $\rho \geqslant 0.34$  g cm<sup>-3</sup>, and a/b = 2.07. Finally, we report a new color study showing that 2002  $CC_{249}$  displays an ultra red surface characteristic of a dynamically Cold Classical trans-Neptunian object.

Key words: Kuiper belt objects: individual ((126719) 2002 CC<sub>249</sub>) – techniques: photometric

#### 1. Introduction

The trans-Neptunian (or Kuiper) belt is structured in four dynamical groups: (i) classical trans-Neptunian Objects (TNOs) are between 40 and 48 au, and are not significantly perturbed by Neptune or captured in a mean-motion resonance with Neptune. Their orbits have low inclinations and are almost circular (typically with eccentricity <0.3, (ii) resonant TNOs are trapped in a resonance with Neptune and thus have had significant interactions with Neptune in the past, (iii) scattered disk TNOs have large inclinations and eccentricities, with perihelia near Neptune's orbit, suggesting they were scattered by Neptune in the past, and (iv) extreme or detached TNOs with highly eccentric orbits present perihelion distances (q > 40 au) beyond the Neptune gravitational influence.

Based on orbital inclination, size, and color studies of objects in the classical belt, at least two sub-populations have been identified (Brown 2001; Levison & Stern 2001; Peixinho et al. 2008): (i) the Hot Classical TNOs are dynamically excited, have high orbital inclination and eccentricity and were likely scattered by the giant planets and captured into the trans-Neptunian population, (ii) the Cold Classical TNOs at low inclinations appear more primordial, are small, and are red (Noll et al. 2008a; Benecchi et al. 2009; Batygin et al. 2011).

Among the Cold Classical population, the separated binary fraction is high, about 20%–25%, but in the other dynamical groups the percentage is only 5%–10% (Noll et al. 2008a). Most of the binary Cold Classicals are wide equal-sized binaries with primary and secondary having comparable sizes. In the trans-Neptunian belt, the contact binary population remains elusive. The first and unique confirmed contact binary is  $2001 \text{ QG}_{298}$  (an object in the 3:2 mean-motion resonance with Neptune) whereas  $2003 \text{ SQ}_{317}$  (a Haumea family member, dynamically Hot Classical) and  $2004 \text{ TT}_{357}$  (an object in the 5:2 mean-motion resonance with Neptune) are likely contact binaries (Sheppard & Jewitt 2004; Lacerda et al. 2014; Thirouin et al. 2017). Surprisingly, none of these objects are

in the dynamically Cold Classical sub-population, where the highest fraction of wide binaries is seen.

 $2002 \text{ CC}_{249}$  is a dynamical Cold Classical TNO with a semimajor axis<sup>3</sup> of 47.44 au, an inclination of 0°84, and an eccentricity of 0.20 (Gladman et al. 2008). Based on *Hubble Space Telescope* images, no companion orbiting 2002 CC<sub>249</sub> was detected (Noll et al. 2008b).

In the following section, we present the light curve of  $2002 \text{ CC}_{249}$  based on observations carried out since 2016. The light curve has a large variability caused by an egg-shaped object or more likely by a binary system in close configuration. We also report new color estimates for this object. Next, we describe our observations and the data reduction techniques. Sections 3 and 4 present and analyze the light curve and the colors of  $2002 \text{ CC}_{249}$ . Finally, we summarize our results in the last section of this paper.

#### 2. Observations and Analysis

We present in situ observations carried out with the Discovery Channel Telescope (DCT) and the 6.5 m *Magellan Telescope* (Baade unit) in 2016 and in 2017.

The DCT is located in Arizona (Happy Jack, United States of America). Our observations were obtained with the Large Monolithic Imager (LMI). This instrument is a  $6144 \times 6160$  pixels CCD for a total field of view of  $12'.5 \times 12'.5$ , and a pixel scale of 0''.12/pixel (Levine et al. 2012).

At the Las Campanas Observatory in Chile, we used one of the *Magellan* Twin Telescopes. The Inamori-Magellan Areal Camera & Spectrograph mounted on the Baade telescope is a wide-field imager with eight  $2048 \times 4096$  pixels CCDs. The short camera mode was selected for a pixel scale of  $0\rlap.{''}20/\text{pixel}$  and a  $27\rlap.{'}4$  diameter field.

The light-curve study was performed at DCT using the VR-filter or r'-filter. The color study was performed with the g'r'i' Sloan filters at the *Magellan-Baade Telescope*, and DCT. Our

Orbital elements from the Minor Planet Center, 2017 August.

**Table 1**Summary of Our Observations

UT-date	Nb.	r <sub>h</sub> (au)	Δ (au)	α (°)	Filter	Telescope
2016 Feb 14	23	38.059	37.334	1.0	VR	DCT
2016 Apr 06	19	38.056	37.066	0.2	VR	DCT
2016 May 11	1 + 1 + 1	38.054	37.312	1.0	g'r'i'	DCT
2016 May 13	16	38.054	37.334	1.1	VR	DCT
2017 Mar 10	12	38.036	37.106	0.5	r'	DCT
2017 Mar 18	38	38.036	37.064	0.3	VR	DCT
2017 Mar 19	3	38.036	37.061	0.3	VR	DCT
2017 Mar 20	20	38.036	37.056	0.3	VR	DCT
2017 Mar 30	67	38.035	37.037	0.0	VR	DCT
2017 Apr 24	2+2+2	38.034	37.116	0.6	g'r'i'	Magellan

**Note.** UT-dates (YYYY/MM/DD), the number of images (Nb.) obtained each night, the heliocentric (rh), and geocentric ( $\Delta$ ) distances in astronomical units (au), the phase angle ( $\alpha$ , in degrees) of the observations, the filter (s) used, and the telescope are reported in this table. Geocentric, heliocentric distances, and phase angle are from the minor planet center ephemeris Generator.

basic observing log is reported in Table 1. The calibration and reduction of our images were performed following the procedure described in Thirouin et al. (2014, 2016). The search for periodicities has been performed with the same techniques mentioned in Thirouin et al. (2017). Finally, the color and solar phase curve studies were performed as per Thirouin et al. (2012). For the color study, the best-fit aperture radius varied between 4 and 5 pixels for the *Magellan-Baade* data and was about 3 pixels for the DCT data.

## 3. Photometric Results

#### 3.1. Color and Solar Phase Curve

Santos-Sanz et al. (2009) observed 2002 CC<sub>249</sub> for color studies with the Very Large Telescope<sup>4</sup> on 2004 March 25 (UT) at a phase angle  $\alpha = 0^{\circ}4$ . They calculated: V - R = $0.51 \pm 0.08$  mag,  $R - I = 0.69 \pm 0.06$  mag,  $V - I = 1.20 \pm 0.06$ 0.07 mag and found a spectral gradient of 22.3  $\pm$  8.5%/100 nm. They also derived the absolute magnitudes in the R- and V-bands using the Bowell formalism and the linear formalism (Santos-Sanz et al. 2009):  $H_V(\text{linear}) = 6.50 \pm 0.06 \text{ mag}$ , and  $H_R(\text{linear}) = 5.99 \pm 0.05 \,\text{mag}$ , and found a R-magnitude of  $21.87 \pm 0.05$  mag. It is important to point out that Santos-Sanz et al. (2009) did not know the light curve of 2002 CC<sub>249</sub>, and thus they have not removed the brightness variation due to rotation for their color estimates. Their data have been obtained over about 20 minutes. With such a short duration, they were not able to notice the large amplitude and slow rotation of 2002 CC<sub>249</sub>.

Most of our data have been obtained with a VR-broadband filter, and thus they are not ideal for color study nor solar phase curve study. However, we have two sets of color data<sup>6</sup> suitable for these studies. Unfortunately, the g'- and i'-bands observed

at DCT have insufficient quality to be included here; only the r'-band will be used for the solar phase curve of 2002 CC249. The phase function is

$$\phi(\alpha) = 10^{-0.4\alpha\beta} \tag{1}$$

where  $\alpha$  is the phase angle and  $\beta$  is the phase coefficient at  $\alpha < 2^{\circ}$ . Based our *Magellan* and DCT data, the range of phase angles is limited with observations of 2002 CC<sub>249</sub> at 0°.6 and 1° for color study. However, by including Santos-Sanz et al. (2009) data, the solar phase curve of 2002 CC<sub>249</sub> is over a phase angle range between 0°.4 and 1°. Based on Smith et al. (2002) and Sheppard (2012), one can convert the Johnson-Morgan-Cousins colors (*BVRI*, used by Santos-Sanz et al. 2009) to the Sloan colors (g'r'i'z'): V - R = 0.59(g'-r') + 0.11, and R - I = 1.00 (r'-i')+0.21. Using previous equations, Santos-Sanz et al. (2009) obtained g'-r' = 0.68 mag, and r'-i' = 0.48 mag.

The absolute magnitude  $(H_{r'})$  is the object's magnitude assuming that the object is at 1 au from the Sun  $(r_h)$  and the Earth  $(\Delta)$  and at  $\alpha = 0^{\circ}$ :

$$H_{r'} = m_{r'}(1, 1, \alpha = 0^{\circ}) = m_{r'} - 5\log(r_h\Delta) - \alpha\beta$$
 (2)

where the corrected r'-band magnitude is  $m_{r'}(1, 1, \alpha)$ . With brightness variations due to rotation and the distance removed, we obtain  $\beta = 0.54 \pm 0.05 \,\mathrm{mag/^{\circ}}$ ,  $H_{r'} = 6.15 \pm 0.05 \,\mathrm{mag}$ (Figure 1). However, the value from Santos-Sanz et al. (2009) is not corrected for brightness variation as the rotational phase for this point cannot be estimated securely. In fact, even if we are able to predict the rotational phase of the Santos-Sanz et al. (2009) data, the propagation of the uncertainty for the rotational period estimate must still be considered. On the other hand, because these two data sets are separated by more than 13 years, we may also have to consider that the light curve has changed over the years due to change in the system geometry (or pole orientation if it is a single object). Therefore, there is an uncertainty of  $\pm 0.4$  mag for the Santos-Sanz et al. (2009) data due to the brightness variation of the object (error bar due to brightness not plotted in Figure 1 for clarity). In conclusion, our phase curve is not optimal and more data are required to provide a clear and secure solar phase curve.

We also use our *Magellan* data set for color study and report:  $g'-i'=1.24\pm0.05$  mag,  $g'-r'=0.97\pm0.06$  mag, and  $r'-i'=0.27\pm0.06$  mag. In conclusion, 2002 CC<sub>249</sub> displays an ultra red surface characteristic of a dynamically Cold Classical TNO based on the Santos-Sanz et al. (2009) study and this work.

# 3.2. Light Curve

Our data set is composed of three isolated nights in 2016 as well as two isolated and three consecutive nights in 2017. During our observations in 2016, only fragments of the light curve of 2002  $CC_{249}$  were obtained. Our longest run was  $\sim$ 3.7 hr, and only one maximum of the curve with an amplitude of about 0.5 mag was observed. Therefore, a long rotational period (P > 8 hr, assuming a double-peaked light curve) was suspected. One maximum and one minimum were observed on UT 2017 March 18, and two minima and one maxima on UT March 30. Both nights allowed us to constrain the rotational period to approximately 12 hr assuming a double-peaked light curve.

<sup>&</sup>lt;sup>4</sup> Santos-Sanz et al. (2009) used the Antu unit at the Very Large Telescope (ESO-VLT, Cerro Paranal, Chile). They used the FORS1 detector and Bessel broadband *BVRI* filters. Details can be found in Santos-Sanz et al. (2009).

<sup>&</sup>lt;sup>5</sup> No Julian Dates are available in Santos-Sanz et al. (2009), but the data are available in the European Southern Observatory (ESO) archive system at: http://archive.eso.org/cms.html.

Data obtained on 2017 March 10 are not considered for the color/phase curve study as the weather conditions were not photometric.

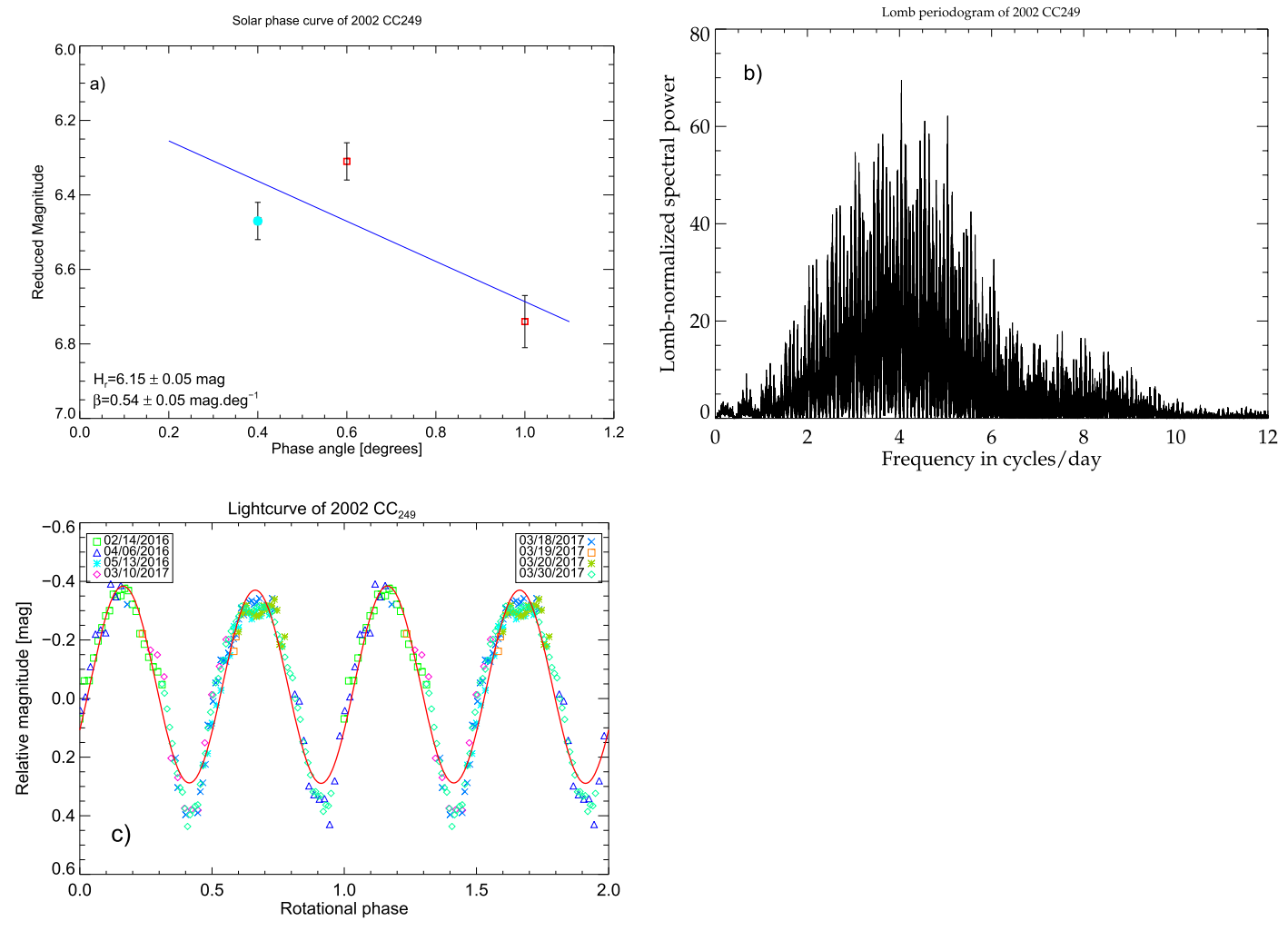


Figure 1. Solar phase curve, Lomb periodogram, and light curve of 2002  $CC_{249}$ . The solar phase curve (a) is plotted using our data (red square), and Santos-Sanz et al. (2009) result (cyan circle). The peak with the highest spectral power of the Lomb periodogram is located at 4.04 cycles/day (b). The double-peaked light curve is plotted over two rotations. The second order Fourier series (red continuous line) is not able to reproduce the V-and U-shape of the curve (c). Error bars are not plotted for clarity, but the typical error bar is  $\pm 0.05$  mag for the photometry.

We applied a light-time correction to our observing runs. The highest peak of the Lomb periodogram is at 4.04 cycles/day (5.94 hr), and the PDM method confirms such a peak (Figure 1). The next step is to select the best option between single- and double-peaked light curve (i.e., period of 5.94 hr or 11.87 hr).

Generally, the albedo contributions are up to 20% for asteroids and TNOs (Degewij et al. 1979; Sheppard et al. 2008; Thirouin et al. 2010). Some TNOs like Eris, Makemake, or Haumea have high geometric albedos between 51% and 96% (Sicardy et al. 2011; Ortiz et al. 2012, 2017). The light curves of Eris and Makemake are mostly flat because they are dominated by the nearly spherical shape and/or pole-on orientation of these objects, whereas in the case of Haumea, the light curve is dominated by Haumea's elongated shape, and the dark red spot contribution is only about 10% (Lacerda et al. 2008; Thirouin 2013). Assuming that 2002 CC<sub>249</sub> has a singlepeaked light curve, albedo variation(s) of about 80% would be required on the object's surface. This scenario is unlikely, and therefore the single-peaked option seems inadequate. Second, by plotting the double-peaked light curve, one can appreciate that there is an  $\sim 0.1$  mag asymmetry between the first and second maxima. In conclusion, the double-peaked option is more adequate for 2002 CC<sub>249</sub>. The double-peaked light curve, assuming a periodicity of 11.87 hr and a full amplitude of  $0.79 \pm 0.04$  mag, is plotted over two cycles in Figure 1. In Table 2, we report the photometry used in this work. The zero phase of the light curve is the date of the object's first image (Table 2).

With such a large light curve amplitude, 2002 CC<sub>249</sub> can be a contact binary system with a non-equator-on configuration assuming two objects with similar sizes or a single very elongated object close to an equator-on configuration (see Section 4 for more details). A light curve with a U-/V-shape at the maximum/minimum of brightness is characteristic of a contact/close binary system with a near equator-on orientation (Sheppard & Jewitt 2004; Lacerda 2011). For 2002 CC<sub>249</sub>, one can note the V-shape at the minima and the second maximum with a U-shape. But, the first maximum displays a sharper peak, and thus the U-shape is not obvious. However, it is important to point out that the first maximum is based on fragmentary data sets obtained in 2016. In Section 4.1, we will discuss the "definition" of the U- and V-shapes.

Table 2
Photometry Used in This Paper

Table 2 (Continued)

Object	Julian Date	Relative magnitude	Error	Object	Julian Date	Relative magnitude	
		(mag)	(mag)	Object	Junuii Dute	(mag)	Error (mag)
2002 CC <sub>249</sub>					2457822.93084	0.38	0.11
	2457432.88848	0.07	0.07		2457822.94353	0.38	0.13
	2457432.89676	-0.06	0.14		2457822.95619	0.15	0.10
	2457432.90608	-0.06	0.04		2457822.96892	-0.01	0.11
	2457432.91436	-0.14	0.03		2457822.98330	-0.11	0.12
	2457432.92265	-0.20	0.03		2457822.99580	-0.20	0.08
	2457432.92979	-0.24	0.03		2457830.81664	0.20	0.05
	2457432.93689	-0.28	0.03		2457830.82097	0.30	0.05
	2457432.94402 2457432.95111	$-0.30 \\ -0.36$	0.03 0.03		2457830.83066	0.40	0.05
	2457432.95824	-0.35 -0.35	0.03		2457830.83544	0.39	0.05
	2457432.96535	-0.35 -0.35	0.03		2457830.84025	0.32	0.06
	2457432.90333	-0.38 -0.38	0.03		2457830.84503	0.29	0.05
	2457432.97957	-0.37	0.03		2457830.85821	0.22	0.05
	2457432.98669	-0.37 $-0.32$	0.04		2457830.86299	0.09	0.05
	2457432.99382	-0.30	0.05		2457830.86780	0.09	0.05
	2457433.00095	-0.22	0.04		2457830.87258	0.01	0.04
	2457433.00922	-0.19	0.04		2457830.87740	-0.05	0.04
	2457433.01751	-0.14	0.04		2457830.88218	-0.06	0.04
	2457433.02579	-0.11	0.04		2457830.88699	-0.13	0.05
	2457433.03407	-0.09	0.05		2457830.89178	-0.13 $-0.13$	0.04 0.04
	2457433.04235	-0.05	0.05		2457830.89659	-0.15 -0.16	0.04
	2457484.73942	-0.02	0.11		2457830.89659 2457830.90138	-0.16 -0.18	0.04
	2457484.74778	0.01	0.16		2457830.90138	-0.18 $-0.20$	0.04
	2457484.75619	0.14	0.16		2457830.90019	-0.20 $-0.22$	0.04
	2457484.76586	0.30	0.13		2457830.91097	-0.22 $-0.27$	0.04
	2457484.77536	0.33	0.13		2457830.92057	-0.27 $-0.31$	0.04
	2457484.78552	0.34	0.10		2457830.92538	-0.29	0.04
	2457484.79505	0.34	0.10		2457830.93017	-0.30	0.05
	2457484.80463	0.43	0.12		2457830.93498	-0.33	0.07
	2457484.81407	0.28	0.17		2457830.93977	-0.33	0.07
	2457484.82355	0.13	0.19		2457830.94457	-0.32	0.04
	2457484.83300	0.04	0.13		2457830.94939	-0.33	0.03
	2457484.84244	-0.01	0.08		2457830.95420	-0.34	0.04
	2457484.85189	-0.11	0.05		2457830.95900	-0.30	0.05
	2457484.86134	-0.22	0.05		2457830.96380	-0.31	0.06
	2457484.87078	-0.23	0.07		2457830.96861	-0.32	0.07
	2457484.88023	-0.22	0.06		2457830.97339	-0.31	0.07
	2457484.88968	-0.39	0.05		2457830.97821	-0.34	0.08
	2457484.89912	-0.35	0.08		2457830.98299	-0.30	0.08
	2457484.90858	-0.39	0.09		2457831.71589	-0.22	0.03
	2457521.67318	0.23	0.04		2457831.74388	-0.16	0.04
	2457521.68144	0.19	0.04		2457831.91506	-0.21	0.04
	2457521.68972	0.08	0.04		2457832.90838	-0.23	0.03
	2457521.69799	0.02	0.03		2457832.91319	-0.28	0.04
	2457521.70626	-0.03	0.03		2457832.91797	-0.29	0.05
	2457521.71453	-0.13	0.03		2457832.92279	-0.32	0.06
	2457521.72279	-0.15	0.03		2457832.92758	-0.30	0.07
	2457521.73104	-0.25 0.24	0.03		2457832.93238	-0.29	0.07
	2457521.73931	-0.24	0.03		2457832.93718	-0.29	0.08
	2457521.74772 2457521.75598	-0.30 0.20	0.03 0.03		2457832.94198	-0.28	0.08
		-0.29			2457832.94677	-0.28	0.03
	2457521.76425 2457521.77250	-0.27 $-0.30$	0.03 0.03		2457832.95159	-0.29	0.04
	2457521.77230	-0.30 -0.28	0.03		2457832.95637	-0.32	0.05
	2457521.78911	-0.28 -0.31	0.03		2457832.96118	-0.30	0.06
	2457521.79737	-0.31 $-0.29$	0.03		2457832.96596	-0.32	0.07
	2457822.85438	-0.29 $-0.17$	0.05		2457832.97078	-0.32	0.07
	2457822.86735	-0.17 -0.15	0.00		2457832.97557	-0.34	0.08
	2457822.88009	-0.13 $-0.07$	0.06		2457832.98037	-0.30	0.08
	2457822.89282	0.20	0.00		2457832.98516	-0.18	0.03
					2457832.98997	-0.18	0.04
	2457822.90551	0.27	0.09		2457832.99476	-0.21	0.04

Table 2 (Continued)

Table 2 (Continued)

(Continued)					
Object	Julian Date	Relative magnitude (mag)	Error (mag)		
	2457842.66890	-0.02	0.03		
	2457842.67372	0.04	0.03		
	2457842.67851	0.10	0.04		
	2457842.68331	0.15	0.04		
	2457842.68810	0.21	0.04		
	2457842.69288	0.26	0.04		
	2457842.69767	0.30	0.04		
	2457842.70247	0.32	0.04		
	2457842.70727	0.38	0.04		
	2457842.71206	0.44	0.04		
	2457842.71684 2457842.72163	0.40 0.38	0.04 0.04		
	2457842.72642	0.38	0.04		
	2457842.72042	0.36	0.03		
	2457842.73602	0.29	0.03		
	2457842.74080	0.23	0.03		
	2457842.74559	0.19	0.03		
	2457842.75038	0.10	0.03		
	2457842.75519	0.05	0.03		
	2457842.75998	-0.01	0.02		
	2457842.76476	-0.05	0.02		
	2457842.76955	-0.07	0.02		
	2457842.77433	-0.10	0.02		
	2457842.77914	-0.13	0.02		
	2457842.78394	-0.19	0.02		
	2457842.78872	-0.20	0.02		
	2457842.79351	-0.23	0.02		
	2457842.79829	-0.24	0.02		
	2457842.80310	-0.26	0.02		
	2457842.80789	-0.28	0.02		
	2457842.81267	-0.32	0.02		
	2457842.81747	-0.31	0.02		
	2457842.82225 2457842.82706	-0.31 $-0.30$	0.02 0.02		
	2457842.82700	-0.29	0.02		
	2457842.83663	-0.29 $-0.30$	0.02		
	2457842.84142	-0.31	0.02		
	2457842.84620	-0.32	0.02		
	2457842.85102	-0.31	0.02		
	2457842.85581	-0.31	0.02		
	2457842.86059	-0.31	0.02		
	2457842.86538	-0.29	0.02		
	2457842.87016	-0.30	0.02		
	2457842.87498	-0.26	0.02		
	2457842.87977	-0.22	0.02		
	2457842.88455	-0.20	0.02		
	2457842.88934	-0.18	0.02		
	2457842.89412	-0.14	0.02		
	2457842.89894	-0.11	0.02		
	2457842.90373	-0.09	0.02		
	2457842.90851	-0.07	0.02		
	2457842.91330 2457842.91808	0.00	0.02 0.03		
	2457842.91808	0.03 0.07	0.03		
	2457842.92289	0.07	0.03		
	2457842.92767	0.13	0.03		
	2457842.93726	0.18	0.03		
	2457842.94204	0.26	0.03		
	2457842.94685	0.32	0.04		
	2457842.95163	0.32	0.03		
	2457842.95642	0.33	0.04		
	2457842.96122	0.33	0.04		
	2457942.06600	0.20	0.04		

2457842.96600

Object	Julian Date	Relative magnitude (mag)	Error (mag)	
	2457842.97081	0.36	0.05	
	2457842.97559	0.37	0.05	
	2457842.98041	0.32	0.05	

Note. Julian date is without light-time correction.

### 4. Analysis

# 4.1. V-shape and U-shape: Definition

Hektor, the largest Jupiter Trojan asteroid, was found to have large amplitude short-term light variations with a characteristic U/V-shaped light curve (Cook 1971). This U/V-shaped rotational light curve results from shadowing and viewing geometry effects from a contact binary viewed nearly equator-on (Hartmann & Cruikshank 1978; Wijesinghe & Tedesco 1979; Weidenschilling 1980). The U/V-shape of a rotational light curve for a contact binary asteroid based on viewing geometry and phase angle effects has been further modeled in detail by several authors (Cellino et al. 1989; Lacerda & Jewitt 2007; Gnat & Sari 2010; Descamps 2015). The U-shape for the maximum and V-shape for the minimum peak of a light curve is apparent for contact binary asteroids viewed near the equator on and at low phase angles, for which the latter occurs for all TNOs.

Here, we present a simple way to determine if a rotational light curve is likely caused by a contact binary object based on the differences in the full-width-at-half-maximum (FWMH) for the maximum (U-shape) and minimum (V-shape) peaks of brightness for the light curve. This analysis allows for a more quantitative approach than simple visual inspection of a light curve, without requiring a detailed model of the light curve. This analysis is based on the fact that the U-shape maxima of the light curve should show a higher FWHM than the V-shape minimum of the light curve if there are differences in the peaks and it is caused by a contact binary. The full peak-to-peak amplitude has been used to estimate the U- and V-FWHM.

We show the FWHM of TNOs with large amplitude light curves ( $\Delta m > 0.15$  mag) from Thirouin et al. (2010, 2012, 2014, 2016), Sheppard (2007), Jewitt & Sheppard (2002) and likely contact binaries from Thirouin et al. (2017), Lacerda et al. (2014), and Sheppard & Jewitt (2004) in Figure 2. In this figure, we plot all four FWHM of these objects: two for the U-FWHM for the maximum and two for the V-FWHM for the minimum. It is clear the non-contact binaries or single objects have all of their peaks' FWHM less than about 0.30 and near each other, whereas the likely contact binaries have U-FWHM greater than about 0.30 and V-FWHM less than about 0.20. The differences between the two types of peaks is usually greater than about 0.1 for their FWHM for the contact binaries, whereas for the non-contact binaries, the differences between the various peaks is less than about 0.05.

It appears the maximum and minimum peaks of single objects have similar FWHM peaks throughout the light curve, whereas the likely contact binaries have significantly different FWHM for their maximum and minimum peaks. In Figure 2, we also report the evolution of the V- and U-FWHM of Hektor with the aspect angle of the system (based on Lacerda & Jewitt

0.04

0.39

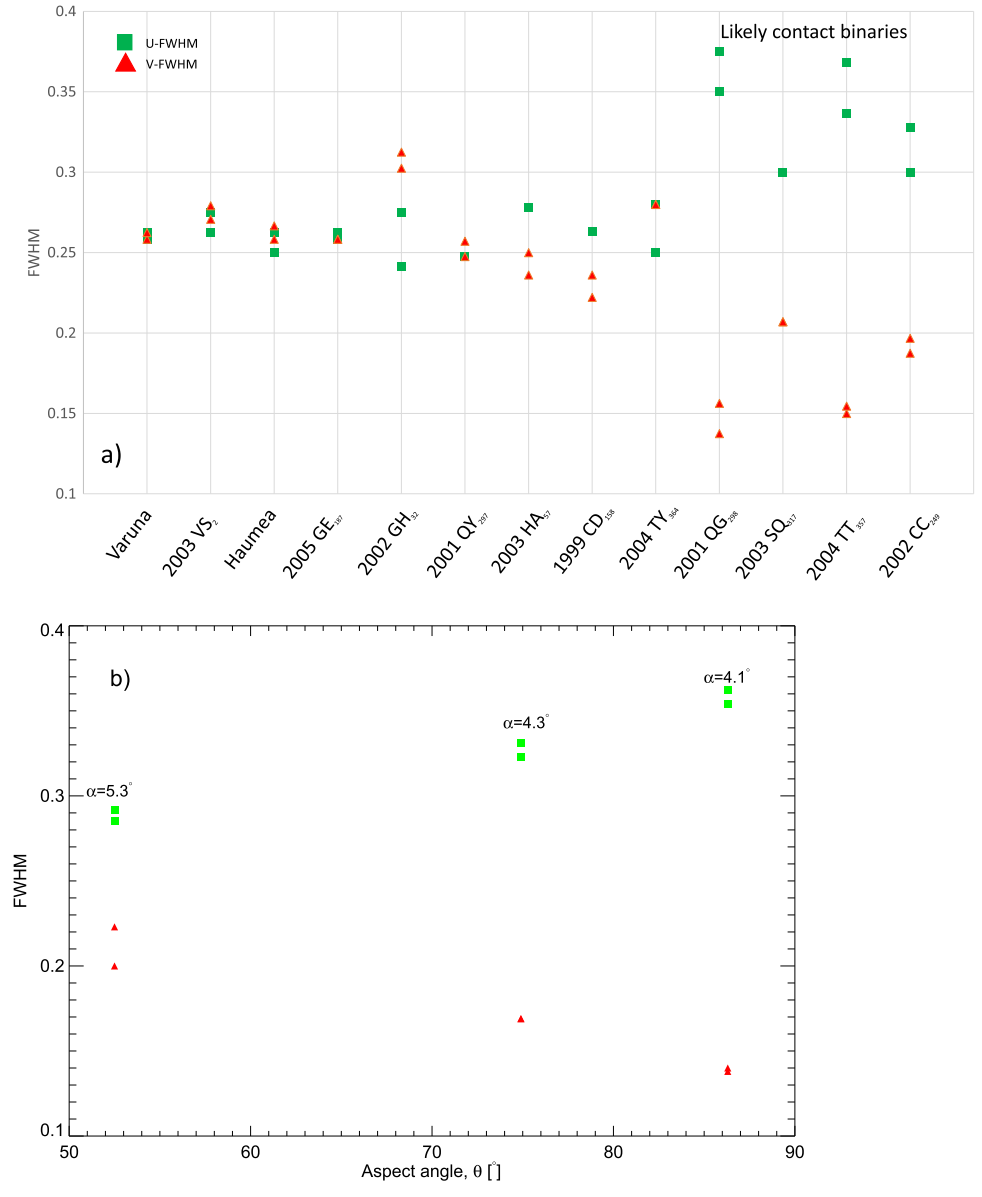


Figure 2. Full width at half maximum (FWHM) of single objects, resolved binaries, and (likely/confirmed) contact binaries. (a) The FWHM of the maxima (U-FWHM) and of the minima (V-FWHM) of several objects are reported. Only double-peaked light curves with an amplitude larger than 0.15 mag are considered. We report the FWHM of both peaks (4 points per object), but in some cases both peaks have the same FWHM. The non-contact binary objects have a U-FWHM  $\leq 0.28$  whereas the (likely/confirmed) contact binaries present a U-FWHM  $\geq 0.30$ . The V-FWHM is  $\leq 0.21$  for the (likely/confirmed) contact binaries. The minima and maxima FWHM peak differences are greater than about 0.1 for contact binaries and less than 0.05 for other objects. 2001 QG<sub>298</sub> is the only confirmed contact binary (Sheppard & Jewitt 2004). (b) The U-/V-FWHM of the Jupiter Trojan Hektor vs. the aspect angle of the system are plotted. Phase angles ( $\alpha$ ) are also indicated for each data set. One can appreciate that the FWHM differences are greater than 0.1 at large aspect angles; the FWHM difference is about 0.1 for an aspect angle around 53°. (Same legend for both plots.)

2007). One can appreciate that at high aspect angles, the differences between the two types of peaks is above 0.1, whereas at an aspect angle of 53°, the difference is near 0.1. For lower aspect angles, the difference is less pronounced.

Again, this is just a simple way to quickly assess if an object's light curve displays a contact binary nature. A full model of the object's likely shape and configuration is needed to fully analyze an object's light curve. In conclusion, we consider that the U/V-shape at the maximum/minimum brightness is significantly different for likely contact binary objects and can be quantitatively looked at by the difference in their FWHM. We find that 2002 CC<sub>249</sub> has a difference of over 0.1 in its U-FWHM versus its V-FWHM, signifying that it is

likely a contact binary like 2001  $QG_{298}$ , 2004  $TT_{357}$ , and possibly 2003  $SQ_{317}$  (Figure 2).

### 4.2. Roche System

The large variability of 2002 CC<sub>249</sub> and its U-/V-shaped light curve is best explained if this object is a contact binary.

Following Leone et al. (1984), the mass ratio and the density of the system are estimated (Figure 3). Two extreme options (min and max) are obtained: (i) a mass ratio  $q_{\min} = 0.6$  and density  $\rho_{\max} = 1 \, \mathrm{g \ cm}^{-3}$  or (ii) a mass ratio of  $q_{\max} = 1$  and density  $\rho_{\max} = 5 \, \mathrm{g \ cm}^{-3}$ . The uncertainty for the mass ratio is  $\pm 0.05$ . For the rest of the study, conservative mass ratios of

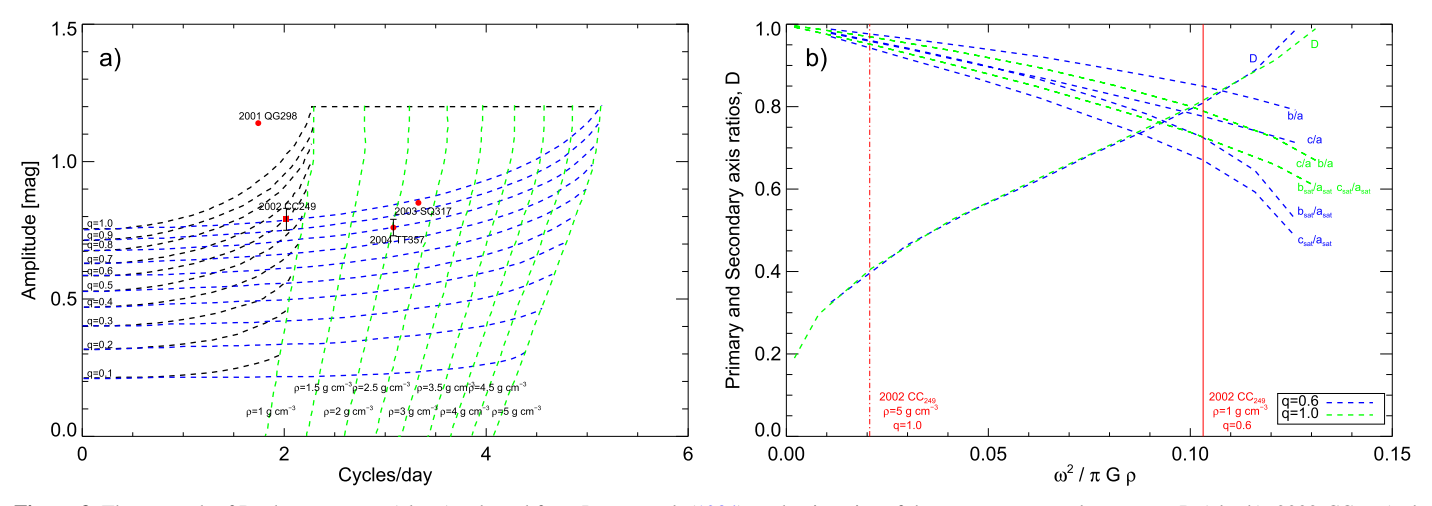


Figure 3. The network of Roche sequences (plot a), adapted from Leone et al. (1984), and axis ratios of the components, and parameter D (plot b): 2002  $CC_{249}$  (red square) can have a mass ratio of 1, and a density of 5 g cm<sup>-3</sup>, or a mass ratio of 0.6 and a density of 1 g cm<sup>-3</sup>. Axis ratios of the primary (b/a, c/a), of the secondary ( $b_{sat}/a_{sat}$ ), and parameter (D) for a mass ratio of 0.6 (blue), and 1 (green). The red dot–dash line is 2002  $CC_{249}$  assuming a mass ratio of 1, and the red continuous line is using a mass ratio of 0.6. See Leone et al. (1984) and Thirouin et al. (2017) for more details about the network of Roche sequences.

 $q_{\min} = 0.6$ , and  $q_{\max} = 1$  will be used (reasons presented in Thirouin et al. 2017).

If 2002 CC<sub>249</sub> is a Roche system with q = 0.6, and  $\rho = 1 \,\mathrm{g\,cm}^{-3}$ , the primary's axis ratios are: b/a = 0.85, c/a = 0.78 ( $a = 125/55 \,\mathrm{km}$ ,  $b = 106/47 \,\mathrm{km}$ , and  $c = 97/43 \,\mathrm{km}$  considering a geometric albedo of 0.04/0.20, and  $H = 6.15 \,\mathrm{mag}$ ). The secondary's axis ratios are:  $b_{\mathrm{sat}}/a_{\mathrm{sat}} = 0.73$ ,  $c_{\mathrm{sat}}/a_{\mathrm{sat}} = 0.67$  ( $a = 117/52 \,\mathrm{km}$ ,  $b = 85/38 \,\mathrm{km}$ , and  $c = 78/35 \,\mathrm{km}$  with an albedo of 0.04/0.20). The value<sup>7</sup> D is 0.81. Therefore, the separation between the components is  $299/132 \,\mathrm{km}$  considering an albedo of 0.04/0.20.

With q=1 and  $\rho=5~{\rm g~cm^{-3}}$ , the axis ratios of the primary are: b/a=0.97, c/a=0.95, and the secondary's axis ratios are:  $b_{\rm sat}/a_{\rm sat}=0.97$ ,  $c_{\rm sat}/a_{\rm sat}=0.95$ , and D = 0.41. A density of 5 g cm<sup>-3</sup> is improbable for an object with a

A density of  $5 \, \mathrm{g \, cm^{-3}}$  is improbable for an object with a diameter in the range 200–400 km and especially for an object at the edge of our solar system. Therefore, the option considering  $\rho = 1 \, \mathrm{g \, cm^{-3}}$  is favored. But, only several light curves obtained at different system's geometries will be required to model the system and improve our estimates.

# 4.3. Jacobi Ellipsoid

A Fourier series (second order, generally able to reproduce light curves due to shape) failed to reproduce the light curve, as the light curve is not a simple sinusoid but has a U-/V-shape to it (Figure 1). This is the reason why we prefer the contact binary hypothesis.

However, we also consider a study that assumes 2002  $CC_{249}$  is a Jacobi ellipsoid.

Following Binzel et al. (1989), the light curve amplitude ( $\Delta$  m) of a Jacobi with a>b>c and in rotation along the c-axis varies as

$$\Delta m = 2.5 \log \left( \frac{a}{b} \right) - 1.25 \log \left( \frac{a^2 \cos^2 \xi + c^2 \sin^2 \xi}{b^2 \cos^2 \xi + c^2 \sin^2 \xi} \right)$$
 (3)

Considering an aspect angle ( $\xi$ ) of 90°, we estimate the object's elongation, a/b = 2.07, and c/a = 0.37 (c/a ratio estimated based on Chandrasekhar 1987). Therefore, using the previous axis ratio estimates and the absolute magnitude reported in this work, we compute: a = 373/167 km, b = 180/81 km, and c = 138/62 km using 0.04/0.20 as albedo values and  $\xi = 90^\circ$ .

With  $\xi=60^{\circ}$ , we derive an elongation larger than 2.31, indicating that the object is unstable to rotational fission due to rotation (Jeans 1919; Sheppard 2004). Therefore, if 2002 CC<sub>249</sub> is a Jacobi ellipsoid, its viewing angle must be between  $76^{\circ}$  and  $90^{\circ}$ .

Assuming an equatorial view and based on Chandrasekhar (1987), we compute the lower density limit as  $\rho \geqslant 0.34 \,\mathrm{g\,cm}^{-3}$ . Such a low value favors an icy composition. This result is compatible with the thermal modeling of TNOs from the *Herschel Space Observatory* and/or *Spitzer*, suggesting a highly porous surface for these outer solar system objects (Lellouch et al. 2013; Vilenius et al. 2014).

### 5. Summary

Based on images carried out using the Lowell's DCT and the *Magellan-Baade Telescope* in 2016 and 2017, we summarize our results as follows.

- 1. 2002 CC<sub>249</sub> has an asymmetric double-peaked light curve with a U-/V-shape at the maximum/minimum of brightness, a periodicity of 11.87 hr, and a peak-to-peak amplitude of 0.79 mag. This extreme variability is best interpreted as a contact binary. 2002 CC<sub>249</sub> is the first contact binary candidate in the dynamically Cold Classical population. This is surprising as the largest fraction of wide binaries is in this population.
- 2. Assuming a contact binary, two main solutions are found: (i)  $q_{\min}=0.6$ , and  $\rho_{\min}=1$  g cm<sup>-3</sup> or (ii)  $q_{\max}=1$ , and  $\rho_{\max}=5$  g cm<sup>-3</sup>.
- 3. Because a density of  $\rho = 5 \text{ g cm}^{-3}$  is doubtful for 2002 CC<sub>249</sub>, we prefer the option with q = 0.6, and  $\rho = 1 \text{ g cm}^{-3}$ . With this option, we find b/a = 0.85, c/a = 0.78 for the primary, and  $b_{\text{sat}}/a_{\text{sat}} = 0.73$ ,  $c_{\text{sat}}/a_{\text{sat}} = 0.67$  for the

 $<sup>\</sup>overline{}^{7}$   $D = (a + a_{\text{sat}})/d$  with the orbital separation (d), and a,  $a_{\text{sat}}$  the primary and secondary longest axes, respectively.

- secondary. We calculate that the components are separated by 299/132 km (using 0.04/0.20 as albedo range).
- 4. If 2002 CC<sub>249</sub> is a Jacobi in hydrostatic equilibrium, we estimate:  $\rho \ge 0.34 \text{ g cm}^{-3}$  and a/b = 2.07, assuming a viewing angle  $\xi = 90^{\circ}$ . Its viewing angle must be between 76° and 90°, if 2002 CC<sub>249</sub> is rotationally stable.
- 5. We report a new color study confirming that 2002  $CC_{249}$  has an ultra red surface, like most Cold Classical objects.
- 6. Contact binaries (likely/confirmed) present maxima of brightness (U-shape) with a larger full width at half maximum (FWHM), and smaller minima of brightness (V-shape) FWHM than single objects. The FWHM of the contact binaries' U-shape is larger than 0.30, whereas other objects have an FWHM ≤ 0.28. The V-shape has an FWHM generally less than 0.21 for the (likely/confirmed) contact binaries. The FWHM difference in minimum and maximum peaks is greater than about 0.1 for contact binaries, and less than 0.05 for other objects, when the viewing angle is near equator-on. In the case of 2002 CC<sub>249</sub>, the U-FWHM are 0.33 and 0.30 whereas the V-FHWM are 0.19 and 0.20 (one value per peak).

We would like to thank the referee for a careful reading of this paper and very useful comments. This research is based on data obtained at the Lowell Observatory's Discovery Channel Telescope (DCT). Lowell operates the DCT in partnership with Boston University, Northern Arizona University, the University of Maryland, and the University of Toledo. Partial support of the DCT was provided by Discovery Communications. LMI was built by the Lowell Observatory using funds from the National Science Foundation (AST-1005313). We acknowledge the DCT operators: Andrew Hayslip, Heidi Larson, Teznie Pugh, and Jason Sanborn. A special thanks to Jason for dealing with some technical difficulties during our DCT runs. This paper includes data gathered with the 6.5 m Magellan-Baade Telescope located at las Campanas Observatory, Chile. A.T. is partly supported by Lowell Observatory funding. The authors acknowledge support from the National Science Foundation, grant No. AST-1734484 awarded to the "Comprehensive Study of the Most Pristine Objects Known in the Outer Solar System."

#### **ORCID iDs**

Audrey Thirouin https://orcid.org/0000-0002-1506-4248 Scott S. Sheppard https://orcid.org/0000-0003-3145-8682

### References

```
Batygin, K., Brown, M. E., & Fraser, W. C. 2011, ApJ, 738, 13
Benecchi, S. D., Noll, K. S., Grundy, W. M., et al. 2009, Icar, 200, 292
Binzel, R. P., Farinella, P., Zappala, V., & Cellino, A. 1989, in Asteroids II
   (Tucson, AZ: Univ. Arizona Press), 416
Brown, M. E. 2001, AJ, 121, 2804
Cellino, A., Zappala, V., & Farinella, P. 1989, Icar, 78, 298
Chandrasekhar, S. 1987, Ellipsoidal Figures of Equilibrium (New York:
Cook, A. F. 1971, NASSP, 267, 155
Degewij, J., Tedesco, E. F., & Zellner, B. 1979, Icar, 40, 364
Descamps, P. 2015, Icar, 245, 64
Gladman, B., Marsden, B. G., & Vanlaerhoven, C. 2008, in The Solar System
   Beyond Neptune, ed. M. A. Barucci et al. (Tucson, AZ: Univ. Arizona
   Press), 43
Gnat, O., & Sari, R. 2010, ApJ, 719, 1602
Hartmann, W. K., & Cruikshank, D. P. 1978, Icar, 36, 353
Jeans, J. H. 1919, Problems of Cosmogony and Stellar Dynamics (Cambridge:
   Cambridge Univ. Press)
Jewitt, D. C., & Sheppard, S. S. 2002, AJ, 123, 2110
Lacerda, P. 2011, AJ, 142, 90
Lacerda, P., & Jewitt, D. C. 2007, AJ, 133, 1393
Lacerda, P., Jewitt, D., & Peixinho, N. 2008, AJ, 135, 1749
Lacerda, P., McNeill, A., & Peixinho, N. 2014, MNRAS, 437, 3824
Lellouch, E., Santos-Sanz, P., Lacerda, P., et al. 2013, A&A, 557, A60
Leone, G., Paolicchi, P., Farinella, P., & Zappala, V. 1984, A&A, 140, 265
Levine, S. E., Bida, T. A., Chylek, T., et al. 2012, Proc. SPIE, 8444, 844419
Levison, H. F., & Stern, S. A. 2001, AJ, 121, 1730
Noll, K. S., Grundy, W. M., Chiang, E. I., Margot, J.-L., & Kern, S. D. 2008a,
   in The Solar System Beyond Neptune, ed. M. A. Barucci et al. (Tucson, AZ:
   Univ. Arizona Press), 345
Noll, K. S., Grundy, W. M., Stephens, D. C., Levison, H. F., & Kern, S. D.
   2008b, Icar, 194, 758
Ortiz, J. L., Santos-Sanz, P., Sicardy, B., et al. 2017, Natur, 550, 219
Ortiz, J. L., Sicardy, B., Braga-Ribas, F., et al. 2012, Natur, 491, 566
Peixinho, N., Lacerda, P., & Jewitt, D. 2008, AJ, 136, 1837
Santos-Sanz, P., Ortiz, J. L., Barrera, L., & Boehnhardt, H. 2009, A&A, 494, 693
Sheppard, S. S. 2004, PhD thesis, Univ. Hawaii
Sheppard, S. S. 2007, AJ, 134, 787
Sheppard, S. S., & Jewitt, D. 2004, AJ, 127, 3023
Sheppard, S. S., Lacerda, P., & Ortiz, J. L. 2008, in The Solar System Beyond
   Neptune, ed. M. A. Barucci et al. (Tucson, AZ: Univ. Arizona Press), 129
Sheppard, S. S. 2012, AJ, 144, 169
Sicardy, B., Ortiz, J. L., Assafin, M., et al. 2011, Natur, 478, 493
Smith, J. A., Tucker, D. L., Kent, S., et al. 2002, AJ, 123, 2121
Thirouin, A. 2013, PhD thesis, Univ. Granada
Thirouin, A., Noll, K. S., Ortiz, J. L., & Morales, N. 2014, A&A, 569, A3
Thirouin, A., Ortiz, J. L., Campo-Bagatin, A., et al. 2012, MNRAS, 424, 3156
Thirouin, A., Ortiz, J. L., Duffard, R., et al. 2010, A&A, 522, A93
Thirouin, A., Sheppard, S. S., Noll, K. S., et al. 2016, AJ, 151, 148
Thirouin, A., Sheppard, S. S., & Noll, K. S. 2017, ApJ, 844, 135
Vilenius, E., Kiss, C., Müller, T., et al. 2014, A&A, 564, A35
Weidenschilling, S. J. 1980, Icar, 44, 807
Wijesinghe, M. P., & Tedesco, E. F. 1979, Icar, 40, 383
```